Photosynth Res (2016) 129:291–305
DOI 10.1007/s11120-016-0297-z

ORIGINAL ARTICLE

Photoacclimation of photosynthesis in the Eustigmatophycean *Nannochloropsis gaditana*

Andrea Meneghesso[1] · Diana Simionato[1] · Caterina Gerotto[1] · Nicoletta La Rocca[1] · Giovanni Finazzi[2] · Tomas Morosinotto[1]

Received: 9 March 2016 / Accepted: 14 July 2016 / Published online: 22 July 2016
© Springer Science+Business Media Dordrecht 2016

Abstract *Nannochloropsis* is an eukaryotic alga of the phylum *Heterokonta*, originating from a secondary endosymbiotic event. In this work, we investigated how the photosynthetic apparatus responds to growth in different light regimes in *Nannochloropsis gaditana*. We found that intense illumination induces the decrease of both photosystem I and II contents and their respective antenna sizes. Cells grown in high light showed a larger capacity for electron transport, with enhanced cyclic electron transport around photosystem I, contributing to photoprotection from excess illumination. Even when exposed to excess light intensities for several days, *N. gaditana* cells did not activate constitutive responses such as nonphotochemical quenching and the xanthophyll cycle. These photoprotection mechanisms in *N. gaditana* thus play a role in acclimation to fast changes in illumination within a time range of minutes, while regulation of the electron flow capacity represents a long-term response to prolonged exposure to excess light.

Electronic supplementary material The online version of this article (doi:10.1007/s11120-016-0297-z) contains supplementary material, which is available to authorized users.

✉ Tomas Morosinotto
tomas.morosinotto@unipd.it

[1] Dipartimento di Biologia, Università di Padova, Via U. Bassi 58/B, 35121 Padua, Italy

[2] Laboratoire de Physiologie Cellulaire et Végétale, UMR 5168, Centre National de la Recherche Scientifique (CNRS), Commissariat à l'Energie Atomique et aux Energies Alternatives (CEA), Université Grenoble Alpes, Institut National Recherche Agronomique (INRA), Institut de Recherche en Sciences et Technologies pour le Vivant (iRTSV), CEA Grenoble, 38054 Grenoble Cedex 9, France

Keywords Acclimation · Microalgae · Cyclic electron flow · Photoprotection · Nonphotochemical quenching

Introduction

Oxygenic photosynthesis catalyzes the conversion of solar light into chemical energy for CO_2 assimilation and release of molecular oxygen. The complex redox activity of photosystems in the presence of oxygen easily induces the production of reactive oxygen species (ROS), leading to oxidative damage of the photosynthetic apparatus (photoinhibition) (Szabó et al. 2005; Murata et al. 2007; Li et al. 2009). This phenomenon becomes particularly relevant when the absorbed radiation exceeds the saturation level of photosynthesis, and thus photochemical reactions do not readily use excitation energy (Barber and Andersson 1992; Demmig-Adams and Adams 2000; Li et al. 2009). To survive and thrive in a highly variable environment, photosynthetic organisms evolved the ability to maximize light-harvesting efficiency when solar radiation is limited and dissipate energy when irradiance exceeds photosynthetic capacity.

In a natural environment, changes in light intensity occur with different rates spanning from seconds to weeks, and photosynthetic organisms therefore have evolved multiple regulatory mechanisms with different activation timescales, enabling responses to short- and long-term variations (Savitch et al. 2001; Walters 2005; Eberhard et al. 2008). The long-term acclimation response involves changes in the composition of the photosynthetic apparatus according to the irradiance intensity (Falkowski and Owens 1980; Falkowski and LaRoche 1991; Zou and Richmond 2000; Walters 2005). In most photosynthetic organisms, this regulation implies a reduction in the chlorophyll (Chl)

content and an increase in photoprotective xanthophylls when exposed to high irradiance (Rodríguez et al. 2005). In some organisms, the photosystem antenna size, i.e., the number of light-harvesting complexes associated with every reaction center, also changes (Falkowski and Owens 1980; Falkowski and LaRoche 1991; Zou and Richmond 2000; Walters 2005). For example, in the green algae *Dunaliella salina,* the diatom *Skeletonema costatum* and most vascular plants, the functional antenna size of photosystems is significantly reduced in response to high irradiance (Smith et al. 1990; Kurasová et al. 2002). However, the same behavior has not been observed in other green algae (*Chlamydomonas reinhardtii* and *Dunaliella euchlora*) and in most diatoms (*Phaeodactylum tricornutum* and *Cyclotella meneghiniana*) where the antenna size in the photosystems is not modulated by light acclimation (Bonente et al. 2012; Lepetit et al. 2012). This heterogeneous response, even within the same phylum, suggests that the acclimation of the light-harvesting apparatus in photosynthetic organisms is species specific.

Another common feature of light acclimation is the modulation of the photosynthetic capacity. The high light-acclimated cells of the diatom *P. tricornutum* and the green algae *C. reinhardtii* showed an increased photosynthetic electron transport rate (Nymark et al. 2009; Bonente et al. 2012). This is correlated with a high light increase in sinks for photosynthetic electron flow, such as the Calvin–Benson cycle enzymes, with RuBisCO being the main target (Fisher et al. 1989; Simionato et al. 2011). The effects of light acclimation were also observed in some cases at the chloroplast ultrastructural level, with the modulation of the number and reorganization of thylakoid membranes (Wilhelm et al. 2014; La Rocca et al. 2015).

While these acclimation responses represent long-term phenomena, requiring the de novo synthesis or degradation of proteins, photosynthetic organisms also possess faster mechanisms to respond to sudden changes in illumination. In this case, photosynthetic organisms activate the dissipation of a fraction of absorbed energy, thereby reducing ROS production. The fastest known mechanism for the modulation of light-harvesting efficiency is called nonphotochemical quenching (NPQ), involving the dissipation of excess energy as heat (Li et al. 2009). In several eukaryotic algae, NPQ activation depends on the presence of a protein called LHCSR/LHCX, as demonstrated in the green microalga *C. reinhardtii,* the picoeukaryote *Ostreococcus tauri*, and some diatoms (Peers et al. 2009; Zhu and Green 2010; Bailleul et al. 2010b; Gerotto and Morosinotto 2013). In different species, the NPQ capacity is modulated under different growth conditions through the regulation of LHCSR/LHCX accumulation (Peers et al. 2009; Zhu and Green 2010; Gerotto et al. 2011; Taddei et al. 2016).

In minutes, strong illumination also activates the synthesis of the xanthophyll zeaxanthin from preexisting violaxanthin through the activation of Violaxanthin de-epoxidase (VDE) (Jahns et al. 2009; Arnoux et al. 2009). The reverse reaction is mediated through the enzyme zeaxanthin epoxidase, leading to the reconversion of zeaxanthin into violaxanthin. Zeaxanthin enhances NPQ and retards the relaxation of this process in the dark, but also plays a direct role in ROS scavenging (Demmig-Adams 1990; Niyogi et al. 1998; Havaux et al. 2007). The Violaxanthin (Vx)–Zeaxanthin (Zx) cycle is widely distributed in photosynthetic organisms spanning from green algae and plants to *eustigmatophytes* and brown algae, and other xanthophyll cycles also mediate similar responses in other organisms, such as the diadinoxanthin (Dd)–diatoxanthin (Dt) cycle in diatoms (Coesel et al. 2008), which plays a major role in the induction of the NPQ in diatoms (Ruban et al. 2004; Lavaud and Kroth 2006).

While the above-mentioned regulatory mechanisms mainly involve PSII, PSI can also be exposed to radiation damage. This photosystem, however, appears to be more sensitive to over-reduction, due to limitation of photosynthesis by CO_2 assimilation, than to excess excitation. PSI over-reduction is counterbalanced by two mechanisms: (i) the large proton gradient generated in high light, as well as redox feedback, slows down the activity of the cytochrome b_6f complex (Joliot and Johnson 2011), leading to oxidation of PSI, due to donor side limitation. (ii) Additionally, activation of cyclic electron flow (CEF) avoids over-reduction of PSI donors and acceptors, thereby contributing to PSI photoprotection (Shikanai 2014). In addition to its role in photoprotection via the proton motive force, CEF reinjects electrons from the acceptor side of PSI to the PQ pool, in parallel to linear electron flow coming from water to NADPH (LEF). CEF thus contributes to proton translocation into the lumen without net NADPH production, thus regulating the ATP/NADPH ratio depending on the metabolic demand (Eberhard et al. 2008; Peltier et al. 2010).

Although these basic regulatory mechanisms are widespread in photosynthetic organisms, differences are seen in different species, likely depending on the colonization of specific ecological niches (Quaas et al. 2014; Goss and Lepetit 2015; La Rocca et al. 2015): For example, it was suggested that the transthylakoid proton gradient, seminal for NPQ activation in plants and chlorophytes, does not play a direct role in diatoms, where the activation of the response only depends on the xanthophyll cycle (Lavaud and Kroth 2006; Goss et al. 2006). Exploring the variability of photosynthesis regulatory responses and understanding how these responses are adapted to different environmental conditions provide a valuable source of information for a better understanding of the physiological role of these

mechanisms. *Nannochloropsis gaditana* is a microalga of the class *Eustigmatophyceae* within *Heterokonta*, a group which also includes diatoms and brown algae (Cavalier-Smith 2004; Riisberg et al. 2009). These species originated from a secondary endosymbiotic event in which a eukaryotic host cell engulfed a red alga and thus have a different evolutionary history with respect to plants and green algae (Archibald and Keeling 2002). In recent years, species belonging to the *Nannochloropsis* genus have gained increasing interest for their potential exploitation for biodiesel production, reflecting the rapid growth rate and accumulation of lipids in these species (Rodolfi et al. 2009; Sforza et al. 2012; Bondioli et al. 2012). Despite this increased attention, information on the *Nannochloropsis* photosynthetic apparatus and its regulation remain elusive. Available studies have shown that *Nannochloropsis* species have a unique pigment composition, presenting only Chl *a* and lacking the other accessory Chl molecules, while presenting violaxanthin and vaucheriaxanthin esters as the most abundant carotenoids (Sukenik et al. 1992; Lubián et al. 2000; Basso et al. 2014). *Nannochloropsis* was shown to modulate its thylakoid membrane organization in response to light intensity for example increasing the relative volume of the chloroplast and the number of stacks during acclimation to low light (Fisher et al. 1996, 1998).

In the present study, the response of *N. gaditana* cells to different growth irradiances was investigated. We found that high light-acclimated cells modulated the composition of their photosynthetic apparatus to increase photosynthetic electron transport, showing an increased contribution from cyclic electron transport. In contrast, no constitutive activation of the xanthophyll cycle and NPQ could be observed, even in the extreme excessive light condition. This shows that these mechanisms play a specific role in response to rapid changes in illumination conditions. On the other hand, changes in both the composition and mode of functioning of the photosynthetic machinery represent the most effective response to chronic exposure to high light.

Materials and methods

Culture conditions

Nannochloropsis gaditana from CCAP, strain 849/5, was grown in sterile F/2 medium containing 32 g l^{-1} sea salts, 40 mM TRIS–HCl, pH 8, and Guillard's (F/2) marine water enrichment solution (Sigma-Aldrich). The cultures were maintained and propagated using the same medium supplemented with 10 g l^{-1} of Plant Agar (Duchefa Biochemie). The growth experiments were performed in Erlenmeyer flasks through mechanical agitation, starting from a preculture grown at 100 µmol of photons m^{-2} s^{-1} maintained in the exponential phase by dilution with fresh medium for at least 2 weeks. To start the acclimation experiment, the precultures were diluted to an optical density (OD) of 0.2 at 750 nm in a final volume of 200 ml and transferred to different light intensities. Illumination was provided over a 16-h photoperiod (16-h light, 8-h dark) at intensities of 10 (Low Light), 100 (Medium Light) and 1000 (High Light) µmol of photons m^{-2} s^{-1}, using a fluorescent lamp or a LED Light Source SL 3500 (Photon Systems Instruments, Brno, Czech Republic). The temperature was maintained at 22 ± 1 °C in a growth chamber. Growth experiments with additional CO_2 were performed using a Multicultivator MC 1000-OD system (Photon Systems Instruments, Czech Republic), in which temperature was maintained at 21 °C and illumination was provided over a 16-h photoperiod (16-h light, 8-h dark) at intensities of 10, 100, and 1000 µmol of photons m^{-2} s^{-1} using an array of white LEDs. In this case, experiments were performed using a F/2 medium enriched to guarantee nonlimiting nutrient conditions (ten times more $NaNO_3$ and NaH_2PO_4 and two times more $FeCl_3 \cdot 6H_2O$ and EDTA). The suspension culture was constantly mixed and aerated through air bubbling. The growth curves in the multicultivator system were initiated using a preculture grown at 100 µmol of photons m^{-2} s^{-1} in 0.25-L Drechsel bottles under continuous air flow enriched with 5 % CO_2. Algal growth was measured through daily changes in the optical density (OD_{750}), and the cell number was monitored using a Cellometer Auto X4 cell counter (Nexcelom Bioscience).

All curves were repeated at least at five independent times. All analyses were performed on the fifth day of the different growth curves when the cells were still actively growing but had enough time to acclimate to different conditions. To assess whether the cells had sufficient time to acclimate to the growth conditions, flask cultures were reinoculated under the same conditions for multiple generations. As shown in Supplementary Fig. S1, cell growth, pigment composition, and functional analyses showed no significant differences with the cells maintained at different light intensities for multiple generations, supporting the conclusion that 5 days were sufficient to activate responses to different light intensities under these culture conditions.

Pigments analysis

Chlorophyll (Chl) and total Carotenoids (Car) were directly extracted from intact cells using 100 % N,N′-dimethylformamide for at least 48 h in the dark at 4 °C after centrifugation of *Nannochloropsis* cells at 15,000×*g* for 10 min. The pigment concentrations were spectrophotometrically determined using specific extinction coefficients (Wellburn 1994). The content of individual carotenoids

was determined using high-pressure liquid chromatography (HPLC), as previously described (Färber and Jahns 1998) To perform this analysis, pigments were extracted from *Nannochloropsis* cell using 80 % acetone after mechanical lysis in a Mini Bead Beater (Biospec Products) with the help of glass beads (150–212 μm in diameter). The HPLC system comprised a reverse phase column (5 μm particle size; 25 × 0.4 cm; 250/4 RP 18 Lichrocart, Darmstadt, Germany) and a diode array detector to record the absorbance spectra (1100 series, Agilent, 141 Waldbronn, Germany). The peaks of each sample were identified based on the retention time and absorption spectrum. The vaucheriaxanthin retention factor was estimated after correcting that of violaxanthin for differences in absorption at 440 nm.

Thylakoid isolation

To obtain isolated thylakoids, *Nannochloropsis* cells were broken using a Mini Bead Beater (Biospec Products), according to the protocol of Basso et al. (2014). The thylakoids in the appropriate buffer were immediately frozen in liquid nitrogen and stored at −80 °C until further use. All steps were performed at 4 °C in dim light. Total pigments were extracted using 80 % acetone, and the chlorophyll concentration of the samples was spectrophotometrically determined.

Spectroscopic analysis

The spectroscopic analysis was performed on the fifth day of growth in vivo using a Joliot-type spectrophotometer (JTS-10, Biologic, France), as previously described for *N. gaditana* cells (Simionato et al. 2013). Changes in the amount of functional photosynthetic complexes were evaluated after measuring the electrochromic shift (ECS) spectral change in intact cells, representing a shift in the pigment absorption bands associated with changes in the membrane potential (Witt 1979). Upon exposure to a saturating single turnover flash, the ECS kinetics present rather complex features including a fast phase (phase a), not kinetically resolved in the measurements, which reflects charge separation in the two photosystems (Bailleul et al. 2010a). It is possible to evaluate the relative ratio of the two photosystems by comparing the amplitude of this phase in the absence and the presence of PSII inhibitors. The PSII contribution was evaluated as the fraction of phase a that was inhibited upon poisoning the algae with DCMU (3-(3,4-dichlorophenyl)-1,1-dimethylurea, 80 μM) and HA (hydroxylamine, 4 mM). These molecules irreversibly block PSII charge separation, respectively, acting as acceptor and donor side inhibitors of PSII. On the other hand, PSI was estimated as the fraction of the signal that was insensitive to these inhibitors [e.g., (Bailleul et al. 2010a)]. ECS measurements were performed in intact cells using a final concentration of 200 × 10^6 cell ml^{-1}. Data were collected as the difference between the signals at 520 and 498 nm (which represent the positive and negative peaks of the ECS signal in *Nannochloropsis*, respectively) to deconvolute this signal from other spectral changes not related to the building of the transmembrane potential (Simionato et al. 2013).

The spectroscopic quantification of the electron that flows through the photosynthetic electron transport chain was performed measuring P_{700} (the primary electron donor to PSI) at 705 nm in intact cells. Analysis was conducted exposing the samples (final concentration 300 10^{6-} cells ml^{-1}) to saturating actinic light (2050 μmol of photons m^{-2} s^{-1}, 630 nm) for 15 s to maximize P_{700} oxidation and reach a steady state. At the end of the treatment, the light was switched off for the P^+_{700} re-reduction to occur subequently in the dark. The total electron flow (TEF), i.e., the sum of all the electron transport processes through PSI, was estimated measuring the P^+_{700} re-reduction rates after illumination in untreated cells. This was done by fitting the kinetics of P^+_{700} re-reduction with a single exponential to calculate the rate constant of P^+_{700} reduction as $1/\tau$. By multiplying this rate constant times the fraction of P_{700} oxidized (which was obtained by comparison with DCMU- and DBMIB-poisoned cells, see below) we evaluate the number of electrons transferred per unit of time electron flux (Simionato et al. 2013). The same procedure was repeated in samples treated with DCMU (80 μM) to evaluate the contribution of cyclic electron flow (CEF) and with DCMU in combination with DBMIB (dibromothymoquinone, 300 μM) to measure any possible residual electron injection into PSI (possibly occurring via redox equilibration with the soluble redox carriers).

The total PSI content of cells in different light regimes was assessed measuring the maximum P^+_{700} signal in cells treated with DCMU and DBMIB at a saturating actinic light (2050 μmol of photons m^{-2} s^{-1}, 630 nm) in an equal number of cells. Under these conditions, re-reduction of P^+_{700} through photosynthetic electron flow is largely slowed down, thereby allowing to evaluate the full extent of photo-oxidizable P_{700} (Alric 2010; Simionato et al. 2013). To confirm that this treatment was appropriate to completely oxidize P_{700}, we repeated this experiment at several light intensities, as shown in Supplementary Fig. S2.

The PSI antenna size was qualitatively assessed after measuring the kinetics of P_{700} oxidation at 705 nm in isolated dark-adapted thylakoids incubated with methyl viologen (375 μM) and ascorbate (2 mM) for 5 min (Swingley et al. 2010; Bonente et al. 2012). The photo-oxidation kinetics was measured upon excitation with

150 μmol of photons m^{-2} s^{-1} of actinic light at 630 nm (a wide range of actinic light were tested as presented in Supplementary Fig. S3). The presence of a strong final electron acceptor, such as methyl viologen, facilitated P_{700} oxidation at a given actinic light. The antenna size was quantified from the rate constant of the kinetics, calculated again assuming a single-exponential character of the kinetics. The thylakoids were analyzed based on a total Chl amount of 40 μg.

Fluorescence measurements

On the fifth day of growth, the microalgae were collected and dark adapted for 20 min to achieve the complete oxidation of the primary electron acceptor Q_A, reaching a state in which all PSII reaction centers are 'open'. Chlorophyll fluorescence was determined in vivo using a Dual PAM 100 (Heinz-Walz, Effeltrich, Germany). Photosynthetic parameters were assessed using a light curve protocol, where the cells were stepwise exposed to increasing light intensities every 1 min. After this light treatment, cells were exposed to dim light for 30 min to estimate the dark recovery of fluorescence. The parameters Fv/Fm, NPQ and qL, were calculated, respectively, as (Fm − Fo)/Fm, (Fm − Fm′)/Fm′ and (Fm′ − F′) Fo′/(Fm′ − Fo′) F′ (Demmig-Adams et al. 2008).

The PSII antenna size was measured according to the fluorescence induction kinetics using a JTS-10 spectrophotometer in the fluorescence mode. Samples with a final concentration of 200 × 10^6 cell ml^{-1} after 20 min of dark adaptation were incubated with DCMU (80 μM) for 10 min to prevent the oxidation of the primary quinone acceptor Q_A. The induction kinetics was measured upon excitation with 320 μmol of photons m^{-2} s^{-1} of actinic light at 630 nm. In the presence of this inhibitor, an average of 1 photon *per* PSII center is absorbed at time *t*, corresponding to 2/3 of the fluorescence increase. This parameter was estimated for every fluorescence induction trace to evaluate the number of absorbed photons by photosystems II, i.e., their antenna size.

Electron microscopy analysis

For transmission electron microscopy analysis, aliquots of algal cultures, sampled on the fifth day, were gently centrifuged (2000×*g*) for 10 min at room temperature, and the pellets were fixed overnight at 4 °C in 3 % glutaraldehyde in 0.1 M sodium cacodylate buffer (pH 6.9) and post-fixed for 2 h in 1 % osmium tetroxide in the same buffer. The specimens were dehydrated in a graded series of ethyl alcohol and propylene oxide and embedded in araldite. Ultrathin sections (800 nm) cut using an ultramicrotome (Ultracut; Reichert-Jung, Vienna, Austria) and stained with uranyl acetate and lead citrate were subsequently analyzed under a transmission electron microscope (TEM, Tecnai G2,FEI, Oregon) at 100 kV.

Results

Light intensity has little influence on *N. gaditana* growth under CO_2-limiting conditions

In the present study, *N. gaditana* cultures were grown in conditions with artificial seawater and atmospheric CO_2, with mechanical agitation and a 16-h light/8-h dark photoperiod. The growth light intensity was instead set to three highly different intensities ranging from 10, 100, and 1000 μmol of photons m^{-2} s^{-1} (hereafter, respectively, referred to as LL, ML, and HL). As shown in Fig. 1a, all cultures have very similar growth kinetics, suggesting that light availability is not a limiting factor under the culture conditions tested.

The cell mortality in the different cultures was also evaluated based on the difference between the cells counted according to the bright field and fluorescence signals, where only Chl-containing living cells were visible. As shown in Fig. 1b, in flask cultures, HL showed clearly a higher number of bleached cells, ranging from 1 to 2 % in LL to 2 % in ML and 14 % in HL. Such a strong increase in the concentration of dead cells suggests that HL cultures experience significant stress associated with intense illumination.

Cells were also cultivated in a photobioreactor with air bubbling and excess nutrients in the medium supply. As shown in Fig. 1c, for ML and HL, higher CO_2 (via air bubbling) and nutrients availability resulted in faster growth compared with LL under the same conditions, confirming that growth of the algae in flask was not limited by light but rather by nutrient availability. Under nonlimiting nutrient conditions, HL cells grew faster than cells grown in flasks but were not able to exploit the additional light energy available with respect to ML, suggesting that these cells achieved light saturation. LL cultures, on the contrary, did not benefit from the additional carbon and nutrient supply, suggesting a light limitation in all conditions.

The increased stress under high light irradiance is consistent with transmission electron microscopy images of microalgae grown under different light intensities (Fig. 2). LL cells are well organized; in the chloroplast thylakoids, these cells consistently form groups of three membranes linearly distributed in the stroma (Fig. 2a, b). In contrast, HL cells, and, to a smaller extent ML cells, showed the presence of storage lamellar vesicles and alterations in the

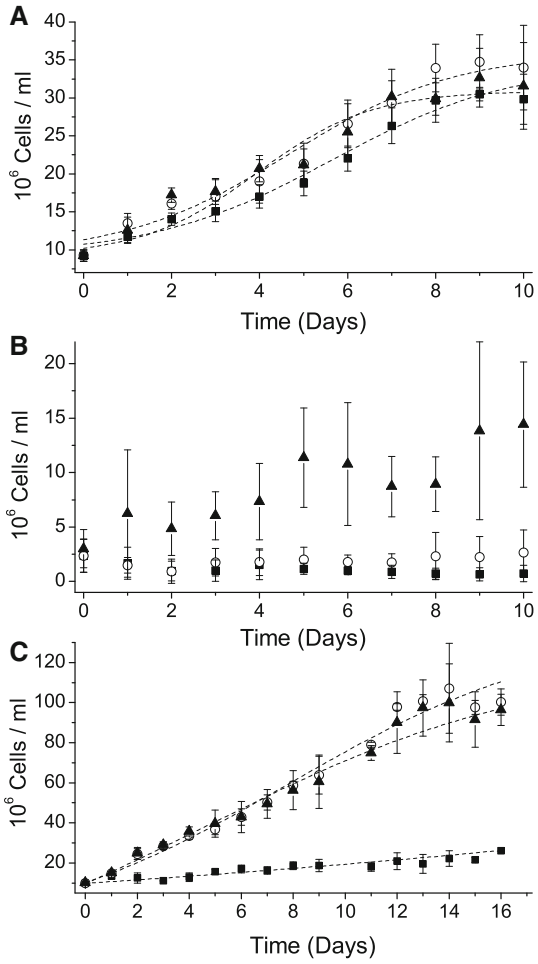

Fig. 1 Cell growth with different illumination. *Nannochloropsis* cells grown under a 16-h photoperiod (16-h light/8-h dark) at intensities of 10 (LL), 100 (ML), and 1000 (HL) μmol of photons m^{-2} s^{-1} are shown, respectively, as *black squares*, *empty circles*, and *black triangles*. **a** The growth rate (Erlenmeyer flasks) in F/2 medium was evaluated after monitoring living fluorescent cells. **b** The dead cells in the cultures shown in **a** were quantified as the difference between cell counts using a bright field and fluorescence microscopy. **c** The growth rate under different light intensities with the external CO_2 supply provided through air bubbling in a Multicultivator MC 1000-OD system in a nutrient-enriched F/2 medium. Note the different *Y* axis between *panels* due to the different growth. All growth curves were repeated at least five independent times. Means and standard deviation (SD) are reported. Although the same external light intensities were applied, the geometry of the growing system was different in experiments with air bubbling, and this light absorbed by the cells was not identical

thylakoid membranes structure (Fig. 2c, e). These effects were better evidenced at higher magnification, where chloroplast membranes displayed a variable number of thylakoids membranes (Fig. 2f). Furthermore, EM pictures showed the presence of a number of highly damaged cells, consistent with higher cell mortality, in HL cultures (not shown).

Modulation of the photosynthetic apparatus composition under different light intensities

Photosynthetic organisms show long-term responses to different light intensities through the modulation of the composition of the photosynthetic apparatus. Among the acclimation strategies to different light regimes, changes in the content or composition of pigments are the most common effects observed. Consistently, *Nannochloropsis* cultures grown under different light conditions showed marked changes in the cell pigment content, and the Chl *a* per cell content was four times higher in LL than in HL (Table 1). In addition, we observed a relative increase in the Car/Chl ratio, consistent with the role of carotenoids in photoprotective responses. The analysis of individual carotenoid species showed that the vaucheriaxanthin content, normalized to Chl, remained stable, and there was a slight increase in canthaxanthin and β-carotene in HL cells. The strongest increase instead involved violaxanthin, which, in absolute values, is majorily responsible for the carotenoid increase observed in HL cells.

Overall, we observed a peculiar behavior of the carotenoids participating in the xanthophyll cycle (violaxanthin, antheraxanthin and zeaxanthin). On one side, these pigments are always present in significant amounts, even in cells growing under light-limiting conditions (1.8 and 2.9 % of total carotenoids are zeaxanthin and antheraxanthin, respectively). In ML cells, the de-epoxidized carotenoids content increased to 3.5 and 6.2 % for zeaxanthin and antheraxanthin, respectively, clearly suggesting some activation of the xanthophyll cycle. However, a further increase in illumination by an order of magnitude (from 100 to 1000 μmol of photons m^{-2} s^{-1}) did not induce any additional conversion of violaxanthin into zeaxanthin, evidenced as the unchanged de-epoxidation index (Table 1). Thus, violaxanthin represented by far the most abundant carotenoid in *Nannochloropsis* cells under all growth conditions, even in cells exposed for days to a high growth light intensity of 1000 μmol of photons m^{-2} s^{-1}.

Chl and carotenoids are bound to photosystem I and II supercomplexes, and the observed changes in the pigment content strongly suggest an altered accumulation of some PS components. To verify this hypothesis, we combined spectroscopic approaches with biochemical quantifications to evaluate the content of all components of the *Nannochloropsis* photosynthetic apparatus. The PSI content in LL-, ML-, and HL-treated cells was quantified after monitoring the P^{+}_{700} absorption signal in cells illuminated with saturating light in the presence of DCMU and DBMIB to inhibit PSI re-reduction (Fig. 3a). The signal dependence on actinic light intensity was also verified to ensure the complete oxidation of the reaction centers in every sample

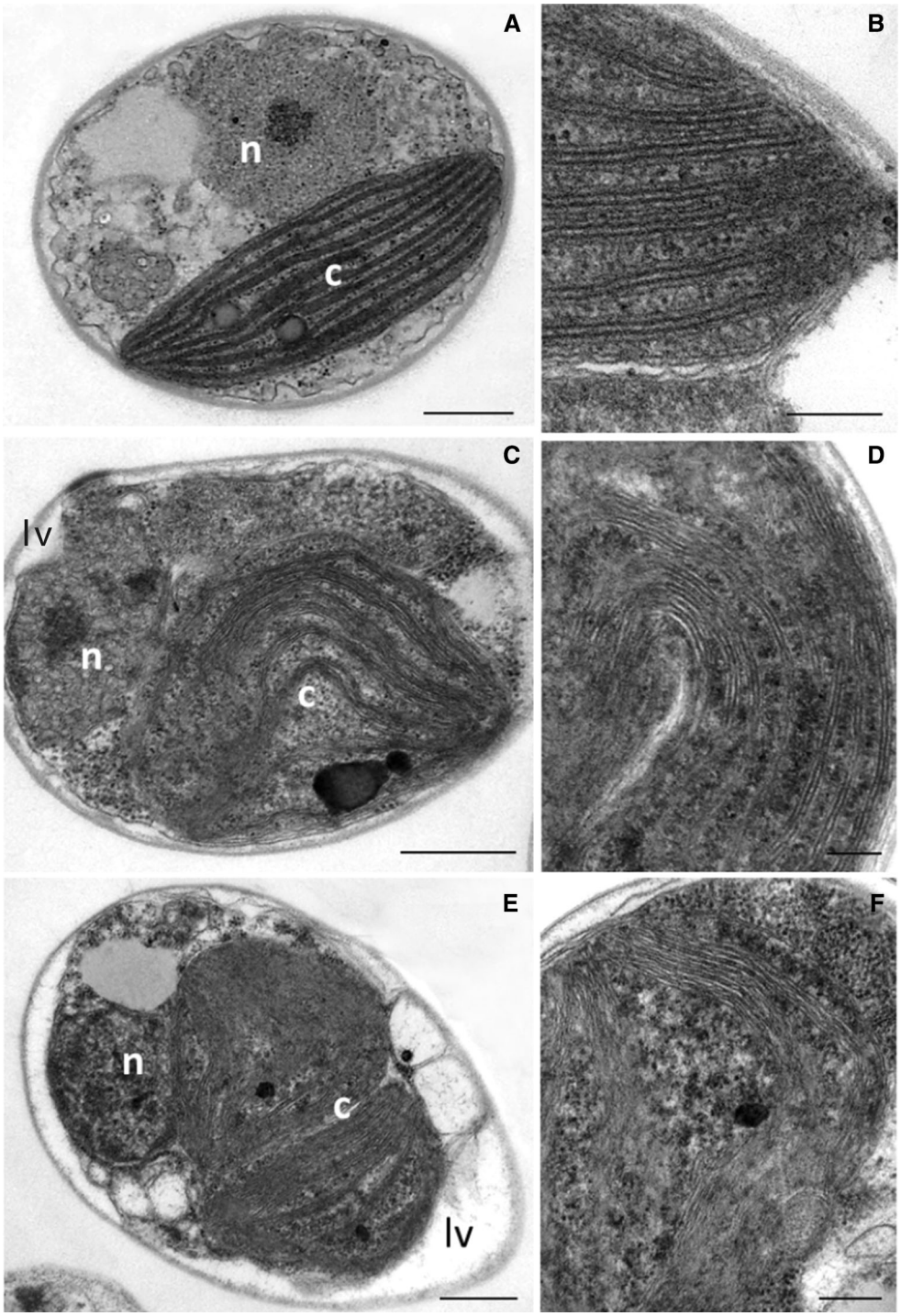

Fig. 2 Transmission electron microscopy of *N. gaditana* cells. Representative transmission electron microscopy of *N. gaditana* cells in LL (**a**, **b**), ML (**c**, **d**), and HL conditions (**e**, **f**). Damaged cells are not shown. *Panels* **b**, **d**, and **f** show magnifications focusing on the thylakoid membrane organization. The organelles are indicated as *n* nucleus; *c* chloroplast; *lv* lamellar vesicles. *Bars* **a**, **c**, **e** = 500 μM; **b**, **d**, **f** = 200 μM

(Supplementary Fig. S2) and rule out any possible shading effect in the P^{+}_{700} quantification. Once verified this prerequisite, the maximal P_{700} signal was exploited to quantify the PSI content in all samples. Figure 3b shows that the PSI content per cell progressively decreased with increasing growth light intensity from LL to ML and HL.

The PSII content is not directly quantifiable using spectrophotometric methods, but can be indirectly assessed

Table 1 Pigment composition of *Nannochloropsis* cells acclimated to different light intensities

	μg Chl/10^6 cells	Tot Car	Violaxanthin	Vaucheriaxanthin	Antheraxanthin	Zeaxanthin	Canthaxanthin	β-carotene	DI
LL	0.151 ± 0.011	35.1 ± 3.4	21.5 ± 2.9	8.2 ± 2.6	1.0 ± 0.2	0.6 ± 0.2	0.3 ± 0.1	5.5 ± 0.3	0.10
ML	0.082 ± 0.005	40.2 ± 3.6	22.9 ± 3.7	8.5 ± 2.1	2.5 ± 0.5	1.4 ± 0.7	0.9 ± 0.2	5.6 ± 0.2	0.20
HL	0.039 ± 0.007	51.1 ± 4.4	32.3 ± 4.6	6.9 ± 1.1	3.5 ± 0.4	2.1 ± 0.3	1.8 ± 0.2	6.8 ± 0.3	0.20

The cells were collected after 5 days of growth under different illumination intensities, when the cells were still actively growing. The carotenoids data are reported as mol/100 mol of Chl *a*, the only chlorophyll species present in *Nannochloropsis*. The data represent the mean ± SD of five independent experiments. The de-epoxidation index (DI) was calculated as (2Z+A)/(V+A+Z)

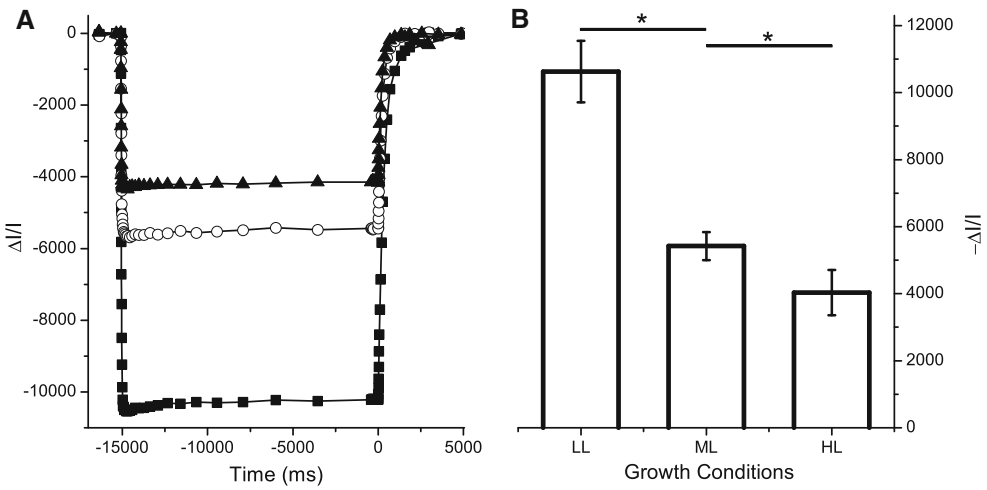

Fig. 3 PSI quantification in *N. gaditana* intact cells. **a** Representative traces of PSI quantification from oxidized P_{700} in the presence of DCMU and DBMIB and a saturating light of 2050 μmol of photons m^{-2} s^{-1}; 300 10^6 cells ml^{-1} were employed for the measurement. Actinic light was verified to be sufficient to reach complete saturation of PSI reaction centers in all cells, as shown in Supplementary fig. S2. LL, ML, and HL conditions are shown, respectively, as *black squares*, *empty circles*, and *black triangles*. **b** Maximal P_{700} oxidation level reached at the steady state during the light treatment **a** in cells acclimated to different light conditions. These *values* represent an indicator of the PSI content. The data are expressed as the mean ± SD, $n = 4$. Significantly different values are indicated by an *asterisk* (ANOVA, p value <0.05)

from the determination of the PSII/PSI ratio using ECS measurements upon exposure to a single turnover flash in the presence/absence of PSII inhibitors (Fig. 4a) (Bailleul et al. 2010a; Simionato et al. 2013). As shown in Fig. 4b, the evaluation of this ratio in different cells showed a decrease in the PSII/PSI ratio in HL-acclimated cells, suggesting that even if the PSI absolute content decreased with illumination intensity in HL cells, the PSII decrease was even larger.

The PSI functional antenna size was qualitatively evaluated measuring the P_{700} oxidation kinetics in thylakoids treated with methyl viologen and ascorbate (Fig. 5a) (Bonente et al. 2012; Iwai et al. 2015) in conditions where the employed actinic light intensity (150 μmol of photons m^{-2} s^{-1}) was limiting for the P_{700} oxidation rate (Supplementary Fig. S3). The employed actinic light indeed was chosen among the lowest actinic light intensities tested, where there is a linear relationship between the amount of light provided and the rate of P_{700} oxidation (Supplementary Fig. S3). Thylakoids from different cells showed different kinetics (Fig. 5), suggesting a gradual decrease of PSI functional antenna size going from LL to HL cells. Compared with ML, LL cells showed a slight increase, while HL showed a more significant decrease of the antenna size, again when related to ML cells.

The PSII functional antenna size was instead quantitatively evaluated based on the kinetics of the increased fluorescence in DCMU-treated cells, again using a limiting illumination (320 μmol of photons m^{-2} s^{-1}, Fig. 6) (Bonente et al. 2012; Simionato et al. 2013). Prior to the measurement, the cells were incubated overnight under dim light to allow the recovery of eventual photo-inhibited PSII reaction centers (Fig. 7a), which otherwise could alter the antenna size determination. The recovery from photodamage was monitored measuring the Fv/Fm parameter that, after the overnight incubation, returned to the maximum values also for HL cells (Fig. 7a). Using this caution, the PSII antenna size showed a clear decrease in response

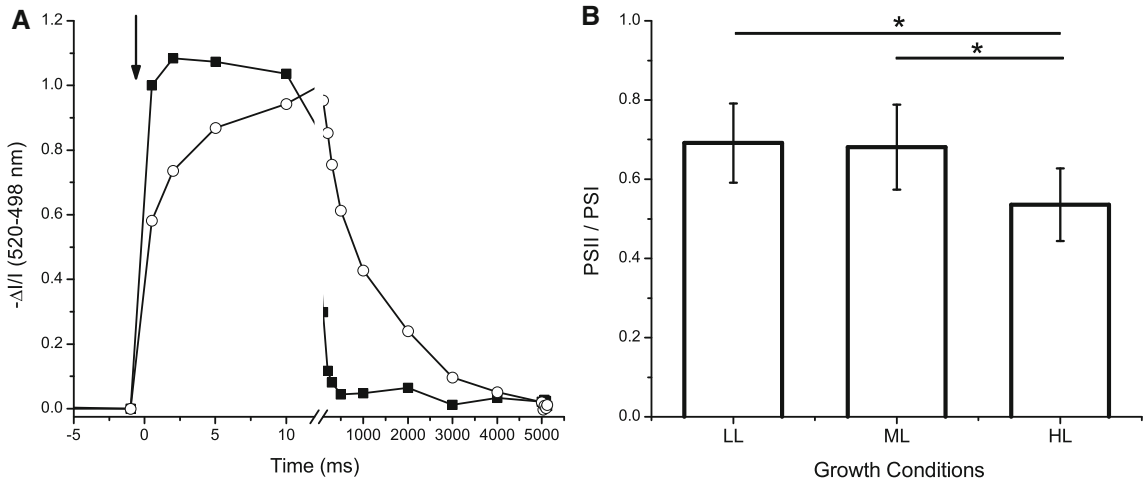

Fig. 4 Evaluation of the PSII/PSI ratio in *Nannochloropsis* cells based on the ECS signal. **a** ECS kinetics in *N. gaditana* cells grown under low light conditions (10 µmol of photons m^{-2} s^{-1}). The ECS signal is presented as the 520 nm minus the 498 nm absorption signal. The signal was induced using a saturating flash (*arrow*). The *solid squares* and *empty circles* represent, respectively, the kinetics of untreated cells (where PSII and PSI both contribute to the ECS signal) and of DCMU and HA-poisoned cells (where only PSI is responsible for the ECS signal). **b** The PSII/PSI ratio obtained from the ECS signal in different acclimated cells with a final concentration of 200×10^6 cell ml^{-1}. The data are expressed as the mean ± SD, $n = 7$. Significantly different values are indicated by an *asterisk* (ANOVA, *p*-value <0.05)

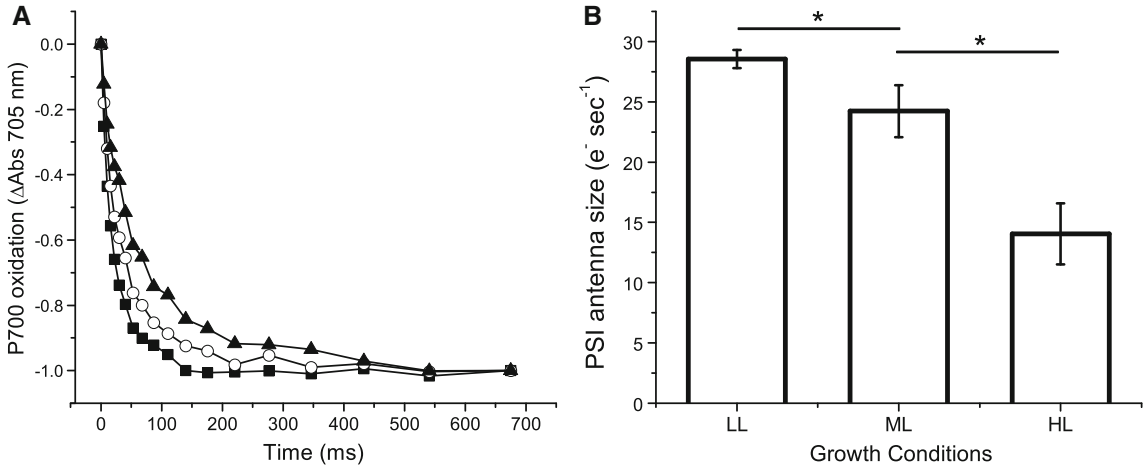

Fig. 5 Modulation of the functional antenna size in PSI. **a** Representative P_{700} oxidation kinetics at 705 nm from thylakoids treated with methyl viologen and ascorbate. The measurements were performed with 150 µmol of photons m^{-2} s^{-1} of actinic light at 630 nm, and the data with other light intensities are shown in Supplementary Fig. S3. LL, ML, and HL conditions are shown, respectively, as *black squares*, *empty circles*, and *black triangles*. **b** Average PSI antenna size for all samples. The data are expressed as the mean ± SD, $n = 4$. Significantly different values are indicated by an *asterisk* (ANOVA, *p*-value < 0.05)

to growth light intensity, suggesting a modulation of the number of light-harvesting complexes associated with each reaction center (Fig. 6). Western blotting analysis with the available antibodies recognizing *Nannochloropsis* proteins confirmed the decrease in high light of VCP, the main antenna complex in *Nannochloropsis* likely associated with PSII (Basso et al. 2014). This was verified upon normalization to the Chl content (Fig. 6c) and the cell number (Supplementary Fig. S4), confirming the results obtained from the functional determination of the PSII antenna size.

Modulation of the efficiency of the photosynthetic apparatus

In order to investigate the consequences on the photosynthetic activity of this rearrangement of the photosynthetic apparatus, we investigated photosynthesis functionality using in vivo fluorescence measurements and time-resolved absorption spectroscopy. The determination of the maximum PSII quantum yield (Fv/Fm) provides an indication of eventual photo-inhibited photosystems. As shown in Fig. 7a, Fv/

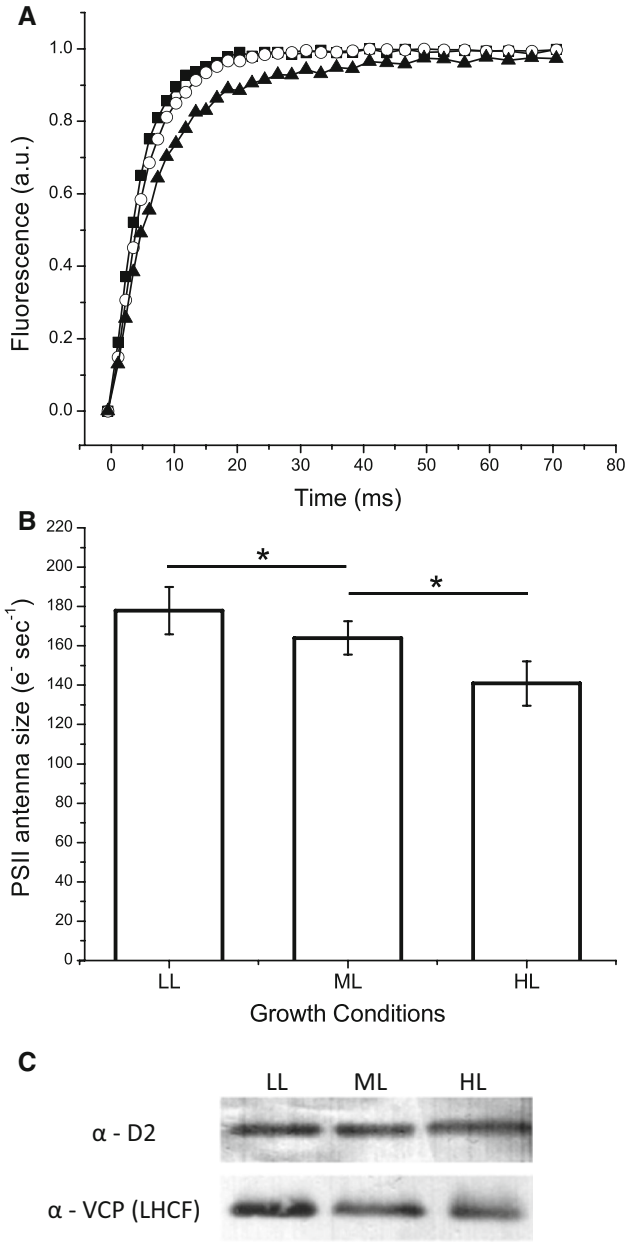

Fig. 6 Modulation of the functional antenna size in PSII. **a** Representative traces of the fluorescence kinetics of DCMU-treated cells in the presence of 320 µmol of photons m^{-2} s^{-1} of actinic light at 630 nm. Prior to the measurement, the cells were incubated overnight under dim light. LL, ML, and HL cells are shown, respectively, as *black squares*, *empty circles*, and *black triangles*. **b** Average PSII antenna size for all samples. The data are expressed as the mean ± SD, $n = 10$. Significantly different values are indicated by an *asterisk* (ANOVA, *p*-value <0.05). **c** Western blotting analysis loading equal amounts of chlorophyll (1 and 0.2 µg Chl for α-D2 and α-VCP, respectively)

Fm decreased from 0.65 in LL to 0.57 in ML and 0.51 in HL cells, suggesting the presence of substantial PSII photodamage in HL, even under ML conditions. PSII activity recovered after an overnight treatment with dim light (10 µmol of photons m^{-2} s^{-1}, Fig. 7a), but not after 1 h of dim light exposure, confirming that the decrease Fv/Fm was due to photoinhibition and not to a slowly recovering NPQ.

The qL parameter, evaluated from fluorescence measurements, allows estimating PSII photochemical efficiency. As shown in Fig. 7b, while LL and ML cells showed a similar dependence of this parameter on the light intensity, HL cells showed a higher photochemical efficiency at all irradiations. This suggests that these cells had a higher ability to use light for photochemistry even if exposed to strong illumination, suggesting the presence of more efficient sinks for electrons from photosynthetic transport chain. The same response for the qL parameter was observed also in cells cultivated with extra CO_2 and nutrients (Supplementary Fig. S5B).

In vivo fluorescence kinetics also provides information on the intracellular dissipation of absorbed energy as heat through a mechanism called Non-Photochemical Quenching (Fig. 7c). LL cells reached higher NPQ values than other cells (Fig. 7c), but most of the additional NPQ did not relax after 30 min of dim light recovery (Fig. 7d). This suggests that the "extra" NPQ mostly reflects photoinhibition rather than enhanced thermal dissipation. Consistent with this, cells grown under different conditions showed no major differences in the fastest NPQ component (qE), which we evaluate as the difference from the last point of light treatment and the first point of the recovery phase (Fig. 7d). A difference was nevertheless seen at the level of NPQ between the different cultures. Indeed, HL cells activated the NPQ response only when exposed to light intensities over 700 µmol of photons m^{-2} s^{-1}, while lower light intensities could trigger this response in the other cells. The same correlation between the NPQ and the light intensity was observed also in cells grown in CO_2− and nutrient-enriched conditions (Supplementary Fig. S5).

NPQ dependence from xanthophyll was investigated by treating cells with a VDE inhibitor (DTT) that affects zeaxanthin synthesis, but not lumen acidification. NPQ was strongly reduced by DTT suggesting a major influence of xanthophyll cycle (Supplementary Fig. S6). Nevertheless, the residual NPQ is still fast activated/deactivated, and thus can be identified as the qE component, dependent from the ΔpH gradient across the membrane (Müller et al. 2001).

Fluorescence-derived signals primarily reflect photosystem II activity, and therefore these data were complemented with measurements of total electron flow monitoring P_{700} re-reduction kinetics after a saturating light treatment that allows evaluating electron transport rates at the level of PSI (Fig. 8a for ML cells, Supplementary Fig. S7 for LL and HL cells). In these samples, the P^{+}_{700} re-reduction in the dark was faster in HL cells with respect to cells acclimated to ML and LL, and maximal total electron flow increased 50 % in HL with

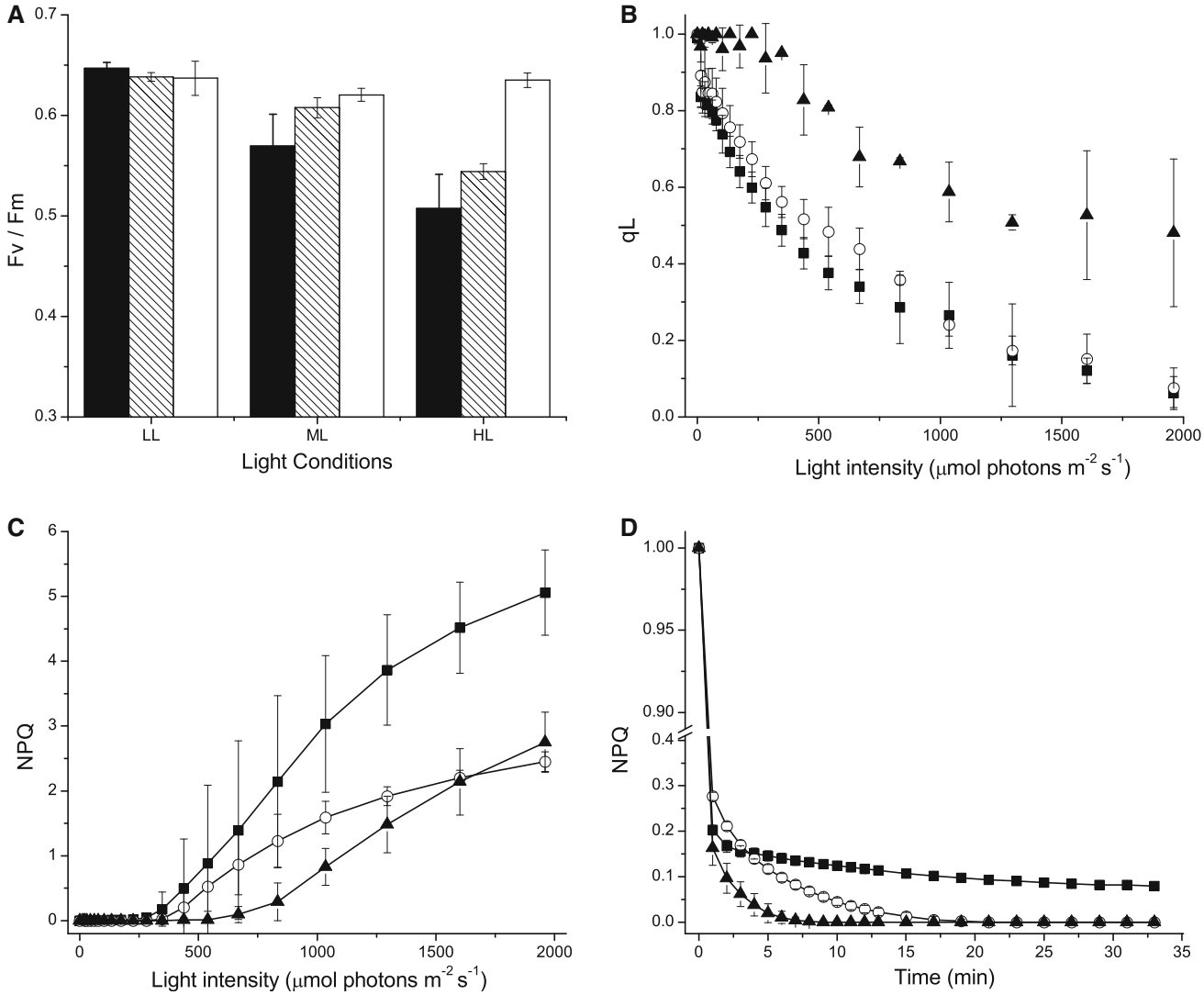

Fig. 7 Photosystem II functionality monitored with PAM fluorimetry. **a** Maximum photosystem II quantum yield (Fv/Fm) in cells grown under different light conditions (LL, ML, and HL) after 20 min of dark adaptation (*dark bars*). Fv/Fm of cells transferred for 1 h or overnight under dim light are reported, respectively, as *dashed* and *white bars*. The data are expressed as the mean ± SD, $n = 2$. **b** Dependence of photochemical efficiency, estimated as the parameter qL, from the illumination intensity. The measurements were performed using 1-min steps of increasing light intensity. **c** NPQ kinetics using 1-min steps of increasing light intensity. **d** NPQ recovery during 30 min of dim light, after the light treatment in **c**. NPQ values are normalized to 1 at the maximal value, before light is decreased. In B-C-D LL, ML, and HL cells are shown as *black squares*, *white circles*, and *black triangles*, respectively. The data are expressed as the mean ± SD, $n = 4$

respect to LL and ML cells (Fig. 8b). Using inhibitors of PSII and cytochrome b_6f (DCMU and DBMIB, respectively), we evaluated the contribution of the linear (LEF) and cyclic (CEF) electron pathways to this total electron transport. As shown in Fig. 8b, under all conditions, PSII inhibition through DCMU dramatically decreased electron transport, suggesting that linear flow is responsible for the largest fraction of electron transport under all conditions. Treatment with both DCMU and DBMIB also inhibits cyclic electron flow around PSI in addition to LEF, facilitating the estimation of the contribution of both pathways. We observed that the CEF contribution was significantly different in the samples analyzed, and while this was hardly detectable in LL cells, its relevance increased in ML and HL cells, reaching around 10 % of all the total electron flow (Fig. 8c).

Discussion

Conserved features and peculiarities in the *Nannochloropsis* acclimation response

Nannochloropsis cultures under different light intensities respond to the environmental conditions through the

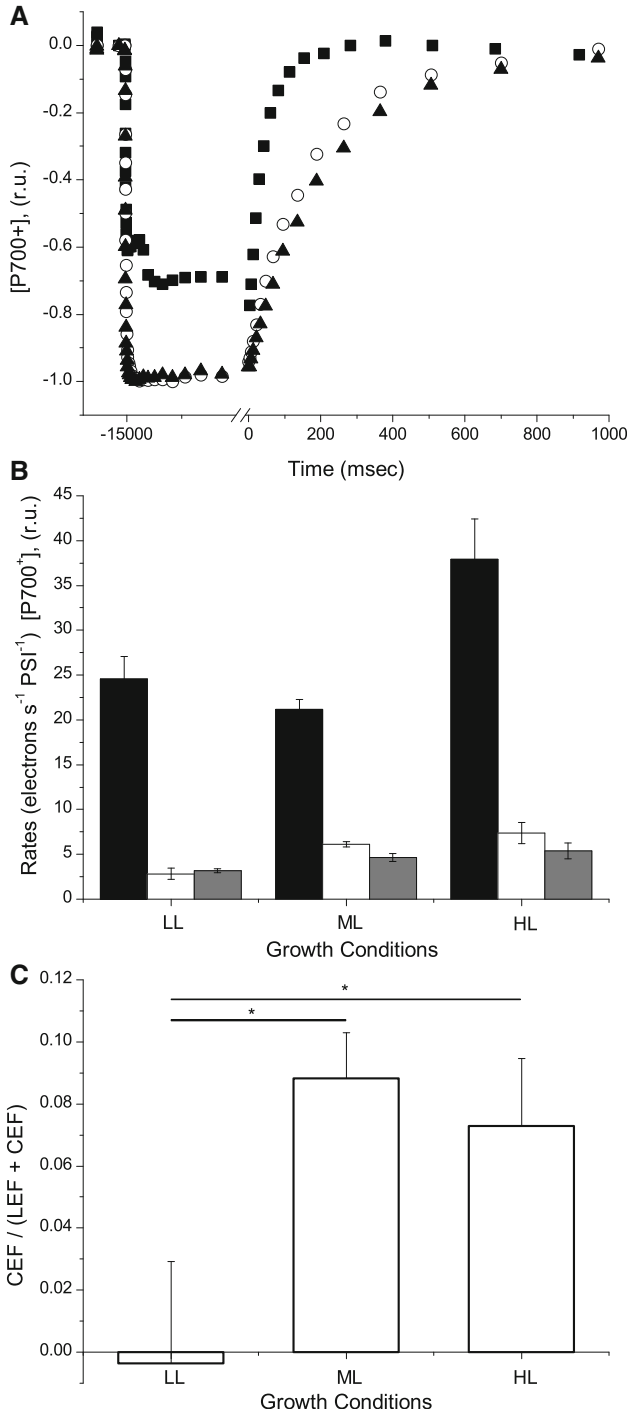

◀**Fig. 8** Maximal PSI electron transport efficiency in cells acclimated to different conditions. **a** P_{700} redox kinetics representing an electron transport quantification experiment. The cells acclimated to 100 µmol of photons m^{-2} s^{-1} (ML) were exposed to a saturating light intensity (2050 µmol of photons m^{-2} s^{-1}) for 15 s prior to the dark recovery kinetics: Untreated cells (*solid squares*), cells treated with DCMU (*open circles*), and cells treated with DCMU and DBMIB (*solid triangles*). The kinetics for LL and HL cells are reported in Supplementary Fig. S7. **b** Electron transport rates evaluated from P_{700} re-reduction kinetics after illumination in different acclimated cells. The data refer to the rates measured in untreated cells (*black column*), DCMU-treated cells (*white column*), and DCMU- and DBMIB-treated cells (*gray column*). The total electron flow values from the three conditions are all significantly different (ANOVA), $n = 4$, $p < 0.05$. **c** Rate of cyclic electron flow (CEF) compared with the sum of linear and cyclic (LEF + CEF). Significantly different values are indicated by an *asterisk* (ANOVA, $n = 4$, p-value <0.05). The data are expressed as the mean ± SD

reorganization of the photosynthetic apparatus and the modulation of its photosynthetic efficiency. *Nannochloropsis* cells acclimated to high light intensities show a decrease in the cell Chl content, reflecting a general decrease in all components of the photosynthetic apparatus, consistent with a reduction of the number of thylakoid membranes (Fig. 2) (Fisher et al. 1998; Lepetit et al. 2012). In high light-treated cells, both PSI and PSII were decreased, but the effect was stronger for PSII, as evidenced by the PSII/PSI ratio (Fig. 4). In fact, while the Chl content per cell decreased to 25 % in HL cells (Table 1), the PSI content per cell was only reduced to 38 % of the LL content (Fig. 3), and P_{700}/Chl ratio in HL showed an approximately 30 % increase (Supplementary Fig. S3B). An even larger decrease was observed for the light-harvesting complexes, as the functional antenna size decreased under HL for both PSI and PSII (Figs. 5 and 6). In the latter case, a diminished antenna content was also biochemically confirmed through Western blotting quantification of the VCP, a major component of PSII antenna in *Nannochloropsis* (Basso et al. 2014).

The seminal study by Falkowski and Owens (Falkowski and Owens 1980) identified two possible strategies used by algal species to respond to changes in growth irradiance, the modulation of the number of reaction centers (called n-type photoacclimation) or the regulation of antenna absorption cross-section serving reaction center, a strategy termed σ-type photoacclimation. These two strategies are not mutually exclusive, as observed here for *N. gaditana,* where cells showed a modulation of photosystem antenna size as well as the reaction center content when exposed to different light intensities. The response of *N. gaditana* is peculiar when compared to previous observation in *C. reinhardtii* and *Arabidopsis thaliana*, where the modulation of antenna size was only observed for PSII, while the PSI antenna composition remained stable (Ballottari et al. 2007; Bonente et al. 2012). Notably, however, the stability of the PSI antenna size in different irradiances has consistently been observed in green algae and plants, while the information for other photosynthetic organisms remains incomplete. LHC associated with PSI in *viridiplantae* shares a common evolutionary origin, and they all belong to a subgroup of antennas called LHCA, whose association with the PSI core complex was shown to be particularly

stable and potentially resulted in the loss of the flexibility required for regulation (Ballottari et al. 2004). *Heterokonta*, like *Nannochloropsis* or diatoms, does not present proteins classified as LHCA and other subunits compose their PSI antenna system (Vieler et al. 2012; Ikeda et al. 2013). Thus, it is possible that with the diversification of photosystem I subunits during evolution in some cases, the ability to form stable super-complexes was selected at the expense of flexibility.

The prolonged exposition of *Nannochloropsis* to strong illumination also influenced the ability to use absorbed light for photochemistry and activate NPQ in response to different illumination intensities (Fig. 7). HL cells showed a higher qL at all actinic light intensities, indicating that the overall modulation of the photosynthetic apparatus enables the cells to exploit higher light more efficiently than LL and ML cells. Moreover, HL cells showed the activation of the NPQ only when exposed to strong light, over 700 µmol of photons m^{-2} s^{-1}. This value is comparable to the average illumination these cells are exposed to, suggesting that these cells do not constitutively activate NPQ under typical growth conditions. This response was also present if nutrients limitation was removed, demonstrating the response was mainly determined from light conditions (Supplementary Fig. S5).

The increased photosynthetic capacity is confirmed by direct measurements of the total electron flow rate using time-resolved spectroscopy in vivo. These measurements show not only an increased capacity to perform electron flow, but also an increased contribution of cyclic electron flow up to 10 % of the total flux. Interestingly, this value is close to the theoretical contribution of CEF needed to reach the optimum ATP/NADPH balance for CO_2 assimilation (Allen 2002). Therefore, it is tempting to propose that the observed changes in the PSI and PSII absorption capacity, as well as in their relative ratio, would not only optimize linear electron flow, but also boost the PSI-driven electron flow alone. This would allow adjusting the NADPH/ATP ratio generated by photosynthesis, as required for optimal photosynthesis. This activation also contributed to maintain the redox state of the electrons carriers connecting PSI and PSII (e.g., the plastoquinone pool) more oxidized, diminishing the dangerous effects of high light on both PSI and PSII. This response would represent the slow acclimation to chronic exposure to high light. Our quantification was performed using saturating light intensity. However, we expect that the difference will be even larger at the growth light intensity, even if LL cells have a larger number of photosystems per cell.

It is also interesting to mention that an increase in cyclic electron flow in response to high light was also observed in cyanobacteria (Herbert et al. 1995; Thomas et al. 2001), suggesting this is not a *N. gaditana* peculiarity, but a response widespread in photosynthetic organisms.

Faster responses would be guaranteed instead by the NPQ and the xanthophyll cycle, involving the conversion of violaxanthin into zeaxanthin. *Nannochloropsis* has the potential for synthesizing large amounts of zeaxanthin, as violaxanthin is the major carotenoid representing ≈60 % of the carotenoids in the cell. However, when cells were chronically exposed to excess light, we observed a strong increase in the total violaxanthin content, which was not constitutively converted into zeaxanthin (Table 1). Overall, the lack of zeaxanthin accumulation upon prolonged exposition to strong illumination and the lack of NPQ induction indicated that HL-acclimated cells do not constitutively activate photoprotection responses. Even if exposed to chronically excess light in *Nannochloropsis* cells, both the NPQ and xanthophyll cycles remain available to respond to further eventual changes in illumination, thereby maintaining the ability to increase photoprotection mechanisms in cells, when needed.

Acknowledgments This work was supported by the ERC (European Research Council) starting Grant BIOLEAP nr 309485. GF acknowledges CNRS Défi (ENRS 2013), the CEA Bioénergies program, and the Human Frontier Science Program nr HFSP0052. The authors would like to thank Vasil D'Ambrosio for the assistance with HPLC and Western blot analyses.

References

Allen J (2002) Photosynthesis of ATP-electrons, proton pumps, rotors, and poise. Cell 110:273–276

Alric J (2010) Cyclic electron flow around photosystem I in unicellular green algae. Photosynth Res 106:47–56

Archibald JM, Keeling PJ (2002) Recycled plastids: a "green movement" in eukaryotic evolution. Trends Genet 18:577–584. doi:10.1016/S0168-9525(02)02777-4

Arnoux P, Morosinotto T, Saga G et al (2009) A structural basis for the pH-dependent xanthophyll cycle in *Arabidopsis thaliana*. Plant Cell 21:2036–2044. doi:10.1105/tpc.109.068007

Bailleul B, Cardol P, Breyton C, Finazzi G (2010a) Electrochromism: a useful probe to study algal photosynthesis. Photosynth Res 106:179–189. doi:10.1007/s11120-011-9704-7

Bailleul B, Rogato A, de Martino A et al (2010b) An atypical member of the light-harvesting complex stress-related protein family modulates diatom responses to light. Proc Natl Acad Sci USA 107:18214–18219. doi:10.1073/pnas.1007703107

Ballottari M, Govoni C, Caffarri S, Morosinotto T (2004) Stoichiometry of LHCI antenna polypeptides and characterization of gap and linker pigments in higher plants photosystem I. Eur J Biochem 271:4659–4665. doi:10.1111/j.1432-1033.2004.04426.x

Ballottari M, Dall'Osto L, Morosinotto T, Bassi R (2007) Contrasting behavior of higher plant photosystem I and II antenna systems during acclimation. J Biol Chem 282:8947–8958. doi:10.1074/jbc.M606417200

Barber J, Andersson B (1992) Too much of a good thing: light can be bad for photosynthesis. Trends Biochem Sci 17:61–66. doi:10.1016/0968-0004(92)90503-2

Basso S, Simionato D, Gerotto C et al (2014) Characterization of the photosynthetic apparatus of the Eustigmatophycean Nannochloropsis gaditana: evidence of convergent evolution in the

supramolecular organization of photosystem I. Biochim Biophys Acta 1837:306–314. doi:10.1016/j.bbabio.2013.11.019

Bondioli P, Della Bella L, Rivolta G et al (2012) Oil production by the marine microalgae Nannochloropsis sp. F&M-M24 and Tetraselmis suecica F&M-M33. Bioresour Technol 114:567–572. doi:10.1016/j.biortech.2012.02.123

Bonente G, Pippa S, Castellano S et al (2012) Acclimation of *Chlamydomonas reinhardtii* to different growth irradiances. J Biol Chem 287:5833–5847. doi:10.1074/jbc.M111.304279

Cavalier-Smith T (2004) Only six kingdoms of life. Proc Biol Sci 271:1251–1262. doi:10.1098/rspb.2004.2705

Coesel S, Oborník M, Varela J et al (2008) Evolutionary origins and functions of the carotenoid biosynthetic pathway in marine diatoms. PLoS One 3:e2896. doi:10.1371/journal.pone.0002896

Demmig-Adams B (1990) Carotenoids and photoprotection in plants: a role for the xanthophyll zeaxanthin. Biochim et Biophys Acta (BBA)-Bioenerg 1020:1–24. doi:10.1016/0005-2728(90)90088-L

Demmig-Adams B, Adams WW (2000) Harvesting sunlight safely. Nature 403(371):373–374. doi:10.1038/35000315

Demmig-Adams B, Adams WW III, Barker DH et al (2008) Using chlorophyll fluorescence to assess the fraction of absorbed light allocated to thermal dissipation of excess excitation. Physiol Plant 98:253–264. doi:10.1034/j.1399-3054.1996.980206.x

Eberhard S, Finazzi G, Wollman F-A (2008) The dynamics of photosynthesis. Annu Rev Genet 42:463–515. doi:10.1146/annurev.genet.42.110807.091452

Falkowski PG, LaRoche J (1991) Acclimation to spectral irradiance in algae. J Phycol 27:8–14. doi:10.1111/j.0022-3646.1991.00008.x

Falkowski PG, Owens TG (1980) Light-Shade adaptation: two strategies in marine phytoplankton. Plant Physiol 66:592–595. doi:10.1104/pp.66.4.592

Färber A, Jahns P (1998) The xanthophyll cycle of higher plants: influence of antenna size and membrane organization. Biochim Biophys Acta - Bioenerg. 1363:47–58. doi:10.1016/S0005-2728(97)00093-5

Fisher T, Shurtz-swirski R, Gepstein S, Dubinsky Z (1989) Changes in the levels of ribulose-l,5-bisphosphate carboxylase/oxygenase (rubisco) in tetraedron minimum (chlorophyta) during light and shade adaptation. Plant Cell Physiol 30:221–228

Fisher T, Minnaard J, Dubinsky Z (1996) Photoacclimation in the marine alga *Nannochloropsis* sp. (Eustigmatophyte): a kinetic study. J Plankton Res 18:1797–1818

Fisher T, Berner T, Iluz D, Dubinsky Z (1998) The kinetics of the photoacclimation response of *Nannochloropsis* sp. (Eustigmatophyceae): a study of changes in ultrastructure and PSU density. J Phycol 34:818–824

Gerotto C, Morosinotto T (2013) Evolution of photoprotection mechanisms upon land colonization: evidence of PSBS-dependent NPQ in late Streptophyte algae. Physiol Plant 149:583–598. doi:10.1111/ppl.12070

Gerotto C, Alboresi A, Giacometti GM et al (2011) Role of PSBS and LHCSR in *physcomitrella patens* acclimation to high light and low temperature. Plant Cell Environ 34:922–932. doi:10.1111/j.1365-3040.2011.02294.x

Goss R, Lepetit B (2015) Biodiversity of NPQ. J Plant Physiol 172C:13–32. doi:10.1016/j.jplph.2014.03.004

Goss R, Ann Pinto E, Wilhelm C, Richter M (2006) The importance of a highly active and DeltapH-regulated diatoxanthin epoxidase for the regulation of the PS II antenna function in diadinoxanthin cycle containing algae. J Plant Physiol 163:1008–1021. doi:10.1016/j.jplph.2005.09.008

Havaux M, Dall'osto L, Bassi R (2007) Zeaxanthin has enhanced antioxidant capacity with respect to all other xanthophylls in Arabidopsis leaves and functions independent of binding to PSII antennae. Plant Physiol 145:1506–1520. doi:10.1104/pp.107.108480

Herbert SK, Martin RE, Fork DC (1995) Light adaptation of cyclic electron transport through photosystem I in the cyanobacterium *Synechococcus* sp. PCC 7942. Photosynth Res 46:277–285. doi:10.1007/BF00020441

Ikeda Y, Yamagishi A, Komura M et al (2013) Two types of fucoxanthin-chlorophyll-binding proteins I tightly bound to the photosystem I core complex in marine centric diatoms. Biochim Biophys Acta 1827:529–539. doi:10.1016/j.bbabio.2013.02.003

Iwai M, Yokono M, Kono M et al (2015) Light-harvesting complex Lhcb9 confers a green alga-type photosystem I supercomplex to the moss *Physcomitrella patens*. Nat Plants 1:14008. doi:10.1038/nplants.2014.8

Jahns P, Latowski D, Strzalka K (2009) Mechanism and regulation of the violaxanthin cycle: the role of antenna proteins and membrane lipids. Biochim Biophys Acta 1787:3–14. doi:10.1016/j.bbabio.2008.09.013

Joliot P, Johnson GN (2011) Regulation of cyclic and linear electron flow in higher plants. Proc Natl Acad Sci USA 108:13317–13322. doi:10.1073/pnas.1110189108

Kurasová I, Cajánek M, Kalina J et al (2002) Characterization of acclimation of Hordeum vulgare to high irradiation based on different responses of photosynthetic activity and pigment composition. Photosynth Res 72:71–83. doi:10.1023/A:1016018900535

La Rocca N, Sciuto K, Meneghesso A et al (2015) Photosynthesis in extreme environments: responses to different light regimes in the Antarctic alga Koliella antarctica. Physiol Plant 153:654–667. doi:10.1111/ppl.12273

Lavaud J, Kroth PG (2006) In diatoms, the transthylakoid proton gradient regulates the photoprotective non-photochemical fluorescence quenching beyond its control on the xanthophyll cycle. Plant Cell Physiol 47:1010–1016. doi:10.1093/pcp/pcj058

Lepetit B, Goss R, Jakob T, Wilhelm C (2012) Molecular dynamics of the diatom thylakoid membrane under different light conditions. Photosynth Res 111:245–257. doi:10.1007/s11120-011-9633-5

Li Z, Wakao S, Fischer BB, Niyogi KK (2009) Sensing and responding to excess light. Annu Rev Plant Biol 60:239–260. doi:10.1146/annurev.arplant.58.032806.103844

Lubián LM, Montero O, Moreno-Garrido I et al (2000) Nannochloropsis (Eustigmatophyceae) as source of commercially valuable pigments. J Appl Phycol 12:249–255

Müller P, Li XP, Niyogi KK (2001) Non-photochemical quenching. A response to excess light energy. Plant Physiol 125(4):1558–1566

Murata N, Takahashi S, Nishiyama Y, Allakhverdiev SI (2007) Photoinhibition of photosystem II under environmental stress. Biochim Biophys Acta 1767:414–421. doi:10.1016/j.bbabio.2006.11.019

Niyogi KK, Grossman AR, Björkman O (1998) Arabidopsis mutants define a central role for the xanthophyll cycle in the regulation of photosynthetic energy conversion. Plant Cell 10:1121–1134. doi:10.1105/tpc.10.7.1121

Nymark M, Valle KC, Brembu T et al (2009) An integrated analysis of molecular acclimation to high light in the marine diatom *Phaeodactylum tricornutum*. PLoS One 4:e7743. doi:10.1371/journal.pone.0007743

Peers G, Truong TB, Ostendorf E et al (2009) An ancient light-harvesting protein is critical for the regulation of algal photosynthesis. Nature 462:518–521. doi:10.1038/nature08587

Peltier G, Tolleter D, Billon E, Cournac L (2010) Auxiliary electron transport pathways in chloroplasts of microalgae. Photosynth Res 106:19–31. doi:10.1007/s11120-010-9575-3

Quaas T, Berteotti S, Ballottari M et al (2014) Non-photochemical quenching and xanthophyll cycle activities in six green algal species suggest mechanistic differences in the process of excess

energy dissipation. J Plant Physiol 172:92–103. doi:10.1016/j.jplph.2014.07.023

Riisberg I, Orr RJS, Kluge R et al (2009) Seven gene phylogeny of heterokonts. Protist 160:191–204. doi:10.1016/j.protis.2008.11.004

Rodolfi L, Chini Zittelli G, Bassi N et al (2009) Microalgae for oil: strain selection, induction of lipid synthesis and outdoor mass cultivation in a low-cost photobioreactor. Biotechnol Bioeng 102:100–112. doi:10.1002/bit.22033

Rodríguez F, Chauton M, Johnsen G et al (2005) Photoacclimation in phytoplankton: implications for biomass estimates, pigment functionality and chemotaxonomy. Mar Biol 148:963–971. doi:10.1007/s00227-005-0138-7

Ruban A, Lavaud J, Rousseau B et al (2004) The super-excess energy dissipation in diatom algae: comparative analysis with higher plants. Photosynth Res 82:165–175. doi:10.1007/s11120-004-1456-1

Savitch LLV, Barker-Åstrom J, Ivanov AGA et al (2001) Cold acclimation of Arabidopsis thaliana results in incomplete recovery of photosynthetic capacity, associated with an increased reduction of the chloroplast stroma. Planta 214:295–303

Sforza E, Simionato D, Giacometti GM et al (2012) Adjusted light and dark cycles can optimize photosynthetic efficiency in algae growing in photobioreactors. PLoS One 7:e38975. doi:10.1371/journal.pone.0038975

Shikanai T (2014) Central role of cyclic electron transport around photosystem I in the regulation of photosynthesis. Curr Opin Biotechnol 26:25–30. doi:10.1016/j.copbio.2013.08.012

Simionato D, Sforza E, Corteggiani Carpinelli E et al (2011) Acclimation of *Nannochloropsis gaditana* to different illumination regimes: effects on lipids accumulation. Bioresour Technol 102:6026–6032. doi:10.1016/j.biortech.2011.02.100

Simionato D, Block MA, La Rocca N et al (2013) The response of *Nannochloropsis gaditana* to nitrogen starvation includes de novo biosynthesis of triacylglycerols, a decrease of chloroplast galactolipids, and reorganization of the photosynthetic apparatus. Eukaryot Cell 12:665–676. doi:10.1128/EC.00363-12

Smith BM, Morrissey PJ, Guenther JE et al (1990) Response of the photosynthetic apparatus in *Dunaliella salina* (green algae) to irradiance stress. Plant Physiol 93:1433–1440

Sukenik A, Livne A, Neori A et al (1992) Purification and characterization of a light-harvesting chlorophyll-protein complex from the marine Eustigmatophyte *Nannochloropsis* sp. Plant Cell Physiol 33:1041–1048

Swingley WD, Iwai M, Chen Y et al (2010) Characterization of photosystem I antenna proteins in the prasinophyte *Ostreococcus tauri*. Biochim Biophys Acta 1797:1458–1464. doi:10.1016/j.bbabio.2010.04.017

Szabó I, Bergantino E, Giacometti GM (2005) Light and oxygenic photosynthesis: energy dissipation as a protection mechanism against photo-oxidation. EMBO Rep 6:629–634. doi:10.1038/sj.embor.7400460

Taddei L, Stella GR, Rogato A et al (2016) Multisignal control of expression of the LHCX protein family in the marine diatom *Phaeodactylum tricornutum*. J Exp Bot 67:3939–3951. doi:10.1093/jxb/erw198

Thomas DJ, Thomas J, Youderian PA, Herbert SK (2001) Photoinhibition and light-induced cyclic electron transport in ndhB(-) and psaE(-) mutants of Synechocystis sp. PCC 6803. Plant Cell Physiol 42:803–812

Vieler A, Wu G, Tsai C-HH et al (2012) Genome, functional gene annotation, and nuclear transformation of the heterokont oleaginous alga Nannochloropsis oceanica CCMP1779. PLoS Genet 8:e1003064. doi:10.1371/journal.pgen.1003064

Walters RG (2005) Towards an understanding of photosynthetic acclimation. J Exp Bot 56:435–447. doi:10.1093/jxb/eri060

Wellburn AR (1994) The spectral determination of chlorophylls a and b, as well as total carotenoids, using various solvents with spectrophotometers of different resolution. J Plant Physiol 144:307–313

Wilhelm C, Jungandreas A, Jakob T, Goss R (2014) Light acclimation in diatoms: from phenomenology to mechanisms. Mar Genomics 16:5–15. doi:10.1016/j.margen.2013.12.003

Witt HT (1979) Energy conversion in the functional membrane of photosynthesis. Analysis by light pulse and electric pulse methods. The central role of the electric field. BBA Rev Bioenerg 505:355–427

Zhu S-H, Green BR (2010) Photoprotection in the diatom *Thalassiosira pseudonana*: role of LI818-like proteins in response to high light stress. Biochim Biophys Acta 1797:1449–1457. doi:10.1016/j.bbabio.2010.04.003

Zou N, Richmond A (2000) Light-path length and population density in photoacclimation of *Nannochloropsis* sp. (Eustigmatophyceae). J Appl Phycol 12:349–354